Biochemistry

pubs.acs.org/biochemistry Article

Cooperative Heteroligand Interaction with G-Quadruplexes Shows Evidence of Allosteric Binding

Shankar Pandey, Yuanyuan Li, Montwaun D. Young, Shankar Mandal, Laichun Lu, Jacob T. Shelley, and Hanbin Mao*

Cite This: https://dx.doi.org/10.1021/acs.biochem.0c00351 Read Online

ACCESS | Metrics & More | Article Recommendations | Supporting Information

ABSTRACT: Although allosteric binding of small molecules is commonplace in protein structures, it is rather rare in DNA species such as G-quadruplexes. By using CD melting, here, we found binding of the small-molecule ligands PDS and L2H2−6OTD to the telomeric DNA G-quadruplex was cooperative. Mass spectrometry indicated a 1:1:1 ratio in the ternary binding complex of the telomeric G-quadruplex, PDS, and L2H2−6OTD. Compared to the binding of each individual ligand to the G-quadruplex, single-molecule mechanical unfolding assays revealed a significantly decreased dissociation constant when one ligand is evaluated in the presence of another. This demonstrates that cooperative binding of PDS and L2H2−6OTD to the G-quadruplex is allosteric, which is also supported by the mass spectra data that indicated the ejection of coordinated sodium ions upon binding of the heteroligands to the G-quadruplex. The unprecedented observation of the allosteric ligand binding to higher-ordered structures of DNA may help to design more effective ligands to target non-B DNA species involved in many critical cellular processes.

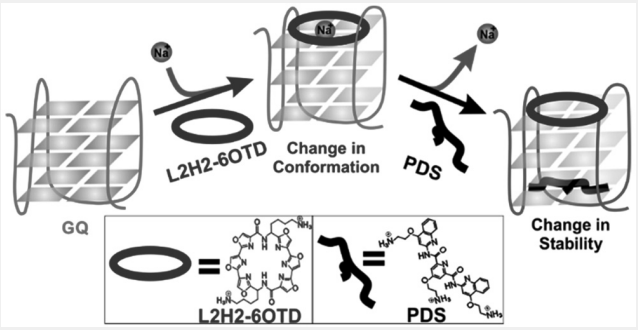

Cooperative binding is a prevalent strategy used by biological systems to alter the binding efficiency of different ligands to the sample substrate.[2] One mechanism of cooperative binding is allosteric binding in which tertiary conformation of the substrate is changed upon binding of the first ligand, which facilitates the binding of the second ligand.[3−5]

Due to the plasticity in a macromolecule, binding of one substrate may change the conformation of the macromolecule, facilitating the binding of other ligands by an effect known as allostery.[6−8] Allostery is often observed in proteins with multitiered structures.[9] However, for nucleic acid structures, allostery is rare.[10] Although some synthetic and natural nucleic acid fragments have shown allosteric effects,[11−14] higher-order natural DNA structures have not demonstrated this behavior to bind small-molecule ligands.

DNA G-quadruplex (see Figure 1) is a higher-order DNA structure found in guanine (G)-rich sequences in vivo.[15] This structure has been shown to participate in many important cellular processes. For example, G-quadruplexes formed in promoter regions can inhibit the expression of oncogenes,[16] which offers a new target for cancer treatment. In one approach exploiting this new target, small-molecule ligands have been developed to bind G-quadruplexes in the oncogene promoters. Recent studies have indeed demonstrated increased inhibitory functions of ligand-bound G-quadruplexes.[17]

The phenomena of cooperativity and allostery are common in proteins and are investigated in the presence of more than two ligands. However, for a noncanonical nucleic acid structure like the DNA G-quadruplex, the investigation of the simultaneous binding of two heteroligands on the G-quadruplex structure has not been reported. In this work, we evaluated the binding of two heteroligands to a human telomeric DNA G-quadruplex by using CD, mass spectrometry, and force spectroscopy methods. By using CD, we found that pyridostatin (PDS) and a telomestatin derivative, L2H2−6OTD, bind to the human telomeric G-quadruplex cooperatively. Mass spectrometry showed the formation of a 1:1:1 ratio of the telomeric G-quadruplex, PDS, and L2H2−6OTD in the ternary complex with the ejection of coordinated sodium ions. The binding affinity measurements from a single-molecule force ramping assay revealed a significantly increased binding of one ligand to the G-quadruplex in the presence of another ligand, which has been used as the key evidence for allosteric binding.[10,18,19] This strongly suggests that the

Received: April 27, 2020
Revised: August 21, 2020
Published: August 24, 2020

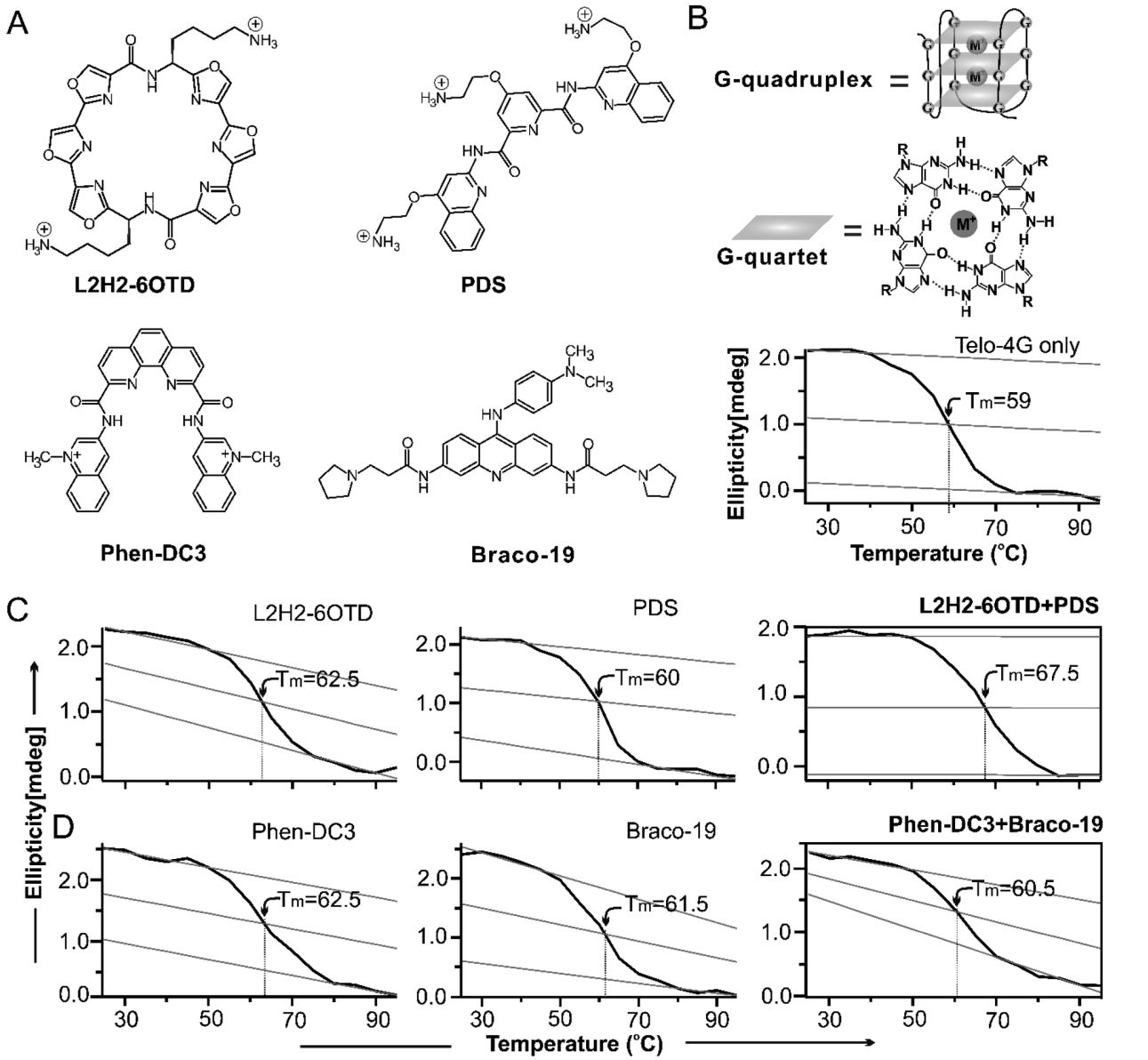

Figure 1. CD melting curves of the DNA Telo-4G fragment with and without ligands. (A) Structures of the telomestatin analogue (L2H2−6OTD), PDS, Phen-DC3, and Braco-19. (B) Top, schematic of a hybrid-1 telomeric G-quadruplex structure and a G-quartet plane. Bottom, CD melting curve of the Telo-4G without any ligand. CD melting curves of the Telo-4G with (C) L2H2−6OTD/PDS ligand(s) (each 5 μM; note there was a significant increase in melting temperature (T_m) when both ligands were present) and (D) Phen-DC3/Braco-19 ligand(s) (each 5 μM, note there was no significant increase in T_m in the presence of both ligands). The melting data at the 290 nm CD signal were retrieved from Figure S2 in the Supporting Information. T_m was determined according to ref 1.

cooperative binding of L2H2−6OTD and PDS to the human telomeric DNA G-quadruplex is allosteric in nature, which is also supported by the ejection of sodium ions revealed by mass spectroscopy. From an in-depth comprehension of allosteric binding of small molecules on G-quadruplex structures, it will provide significant benefit in the development of more selective, potent, and effective allosteric drugs.

MATERIALS AND METHODS

Materials. DNA oligomers were purchased from Integrated DNA Technologies (IDT, IA). Enzymes and plasmids needed for the synthesis of DNA constructs were purchased from New England Biolabs (NEB, England). Streptavidin- or antidigoxigenin-coated polystyrene beads were purchased from Spherotech (Lake Forest, IL). PDS was a gift from Dr. Shankar Balasubramanian at the University of Cambridge; telomestatin analogue, L2H2−6OTD, was a gift from Dr. Kazuo Nagasawa at Tokyo University of Agriculture and Technology. Phen-DC3 was a gift from Dr. Laurence Hurley at the University of Arizona. Braco-19 was purchased from Sigma-Aldrich [$\geq$ 96% (HPLC)].

Preparation of DNA Constructs. The Telo-4G sequence (5′-TTAGGGTTAGGGTTAGGGTTAGGGTTA-3′) was sandwiched between two dsDNA handles (2028 bp and 2391 bp) (see Figure S1 for details). The 2028 bp handle was prepared by the PCR of a pBR322 plasmid template using a 5′-end biotinylated reverse primer, 5′-GCA TTA GGA AGC AGC CCA GTA GTA GG and a forward primer, 5′-AAA ATC TAG AGG CTA CAC TAG AAG GAC AGT ATT TG. Then, the PCR product was digested by using the XbaI enzyme. The

https://dx.doi.org/10.1021/acs.biochem.0c00351
Biochemistry XXXX, XXX, XXX−XXX

biotinylated 2028 bp handle was ligated with the Telo-4G fragment that was flanked by two oligos (underlined), 5′-CTA GAC GGT GTG AAA TAC CGC ACA GAT GCG TTA GGG TTA GGG TTA GGG TTA GGG TTA GCC AGC AAG ACG TAG CCC AGC GCG TC-3′. The second handle (2391 bp) was prepared by the SacI and BsaI-HFv2 digestions of the PCR amplified λ-DNA (primer sequences: SacI primer, 5′-AAA AAA AAG AGC TCC TGA CGC TGG CAT TCG CAT CAA AG-3′ and BsaI primer, 5′-AAA AAA AAG GTC TCG CCT GGT TGC GAG GCT TTG TGC TTC TC-3′). This handle was labeled with digoxigenin (Dig) at the SacI-digested overhang by using 1 nM Dig-dUTP (Roche) and terminal transferase. The 2391 bp handle was finally ligated with the biotinylated DNA through the BsaI site. The DNA construct thus prepared was purified by agarose gel, dissolved in 1 mM Tris (pH 7.4) after ethanol precipitation, and then stored at −20 °C.

Single-Molecule Mechanical Unfolding of the Telo-4G Construct with and without Ligands. Single-molecular investigations were performed with a home-built dual-beam laser tweezers instrument.[20−22] All experiments were performed at ∼23 °C in a 10 mM Tris buffer containing 100 mM KCl at pH 7.4. The antibody-coated 2.10 μm polystyrene bead was incubated with the Telo-4G DNA sample prepared above before the single-molecular experiments. The DNA incubated bead and the streptavidin-coated bead were separately captured by two laser beams. The DNA construct was then tethered between the two beads through digoxigenin-antibody−digoxigenin and biotin−streptavidin interactions. One of the laser foci was fixed while the other was movable by controlling the laser beam. The tethered DNA was stretched with the two beads moving apart. The tension in the DNA tether was recorded in the force−extension (F-X) curves at 1 kHz with a loading rate of ∼5.5 pN/s through a LabView program (National Instruments, Austin, TX). Whether a molecule is single or not was determined by the observation of the ∼65 pN plateau in F-X curves. The data (F-X curves) were filtered through a function of Savitzky−Golay with a time constant of 10 ms in the Matlab program (The MathWorks, Nattick, MA). Mechanical stability of G-quadruplexes formed in the Telo-4G with or without a ligand or a ligand pair was determined by the unfolding force of the G-quadruplex in the F-X curves. The ligand-bound G-quadruplex population was determined by the difference in the mechanical stabilities. To increase the efficiency of data collection for ligand-bound G-quadruplexes, the concentration of each ligand (see figure captions for values) was chosen as high as possible (PDS: 100 nM; L2H2−6OTD: 5 nM) without causing noise in F-X curves, which is due to nonspecific binding of the ligand to the duplex DNA handles.

Evaluation of Thermodynamic Stabilities of the Telo-4G with and without Ligands. One mM stock solution of oligonucleotides, telomeric 4G (5′-TTAGGGTTAGGGTTAGGGTTAGGGTTA-3′), was prepared in DNase-free water. Further dilutions were carried out in phosphate buffer (5 mM K_2HPO_4 and 2 mM KH_2PO_4) containing 100 mM KCl at pH 7.4. Before CD measurement in a JASCO-810 spectropolarimeter (Easton, MD), the DNA samples were heated at 95 °C for 5 min and gently cooled from 95 °C to room temperature. A 1.0 mm path-length cuvette was prepared by the addition of 200 μL (5 μM) of the annealed DNA solution without or with each ligand (5 μM) in a ligand pair or with both ligands of the same concentration (5 μM each). CD spectra were collected at constant temperatures ranging from 25 to 95 °C. Each measurement was carried out in triplicate. Melting temperatures at a 290 nm CD signal were calculated according to the procedure described in literature.[1]

Force-Pumping/Force-Probing Experiments. This approach was designed to investigate the dynamic binding of ligands to the telomeric G-quadruplex.[23] First, the DNA construct was stretched mechanically until a G-quadruplex was unfolded. The DNA was then relaxed by a rapid force jump to 0 pN, allowing refolding of the G-quadruplex structure in subsequent incubations at 0 pN. The refolding of the G-quadruplex was revealed by a rupture event in the next cycle of the stretching process starting at 10 pN, which was achieved by a second force jump in 10 ms. The two force jumps ensure no refolding of the quadruplex structure during stretching and relaxing at the low force region (<10 pN). This procedure can measure events as fast as 10 ms. By differentiating free and ligand-bound G-quadruplexes using rupture forces, we measured the formation kinetics of telomeric G-quadruplexes, as well as the binding kinetics of the PDS (500 nM) and L2H2−6OTD (100 nM) to the G-quadruplex with 0−30 s of incubation time. During the deconvolution of ligand-free and ligand-bound populations, we first fit the two populations in each rupture force histogram using a two-peak Gaussian function (Figures S8 and S9). The overlapping areas between the two populations were then randomly assigned to each of the species according to the ratio of the two species determined by the two-peak Gaussian fitting in each bin of a particular rupture force histogram.

Data Analysis. The change in extension (Δx) at a particular force (F) was calculated as the extension difference between the stretching and the relaxing traces at that force. The resulting Δx at this force was then converted to the change in contour length (ΔL) using the following wormlike-chain (WLC) model:[24,25]

$$\Delta x/\Delta L = 1 - 1/2(k_B T/FP)^{1/2} + (F/S) \quad (1)$$

where Δx is the change in end-to-end distance (or extension) between the two optically trapped beads, ΔL is the change in contour length, k_B is the Boltzmann constant, T is absolute temperature, P is the persistent length of dsDNA (50.8 nm), and S is the stretching modulus (1243 pN).[26]

High-Resolution Mass Spectrometry (HRMS) Measurements. High-resolution mass spectra of the G-quadruplex forming sequences (5 μM in 1 mM Tris-HCl buffer, pH 7.4) and stabilizing ligands (PDS and L2H2−6OTD, each 5 μM) were obtained with an Orbitrap-based mass spectrometer (Q Exactive, Thermo Scientific, Bremen, Germany) via nano-electrospray ionization (nESI). Nanospray emitters with tip diameters of ca. 0.6 μm were produced in-house from quartz tubes (1.0 mm o.d., 0.70 mm i.d., Sutter Instruments, Novato, CA) with a laser-based pipet puller (P-2000, Sutter Instruments, Novato, CA). Annealed G-quadruplex and ligands samples were prepared to a final concentration of 5 μM in 1 mM potassium chloride and 100 mM trimethylammonium acetate (TMMA) buffer solution. Nanoelectrospray was initiated by applying a potential of ca. 0.8 kV to a platinum wire inserted into the capillary and in direct contact with the sample solution.

Mass spectra were recorded in the negative-ionization mode with a scan range of m/z 500−3000, a mass resolving power setting of 140 000, inlet capillary desolvation temperature of 60 °C, and an automatic gain control (AGC) target value of 1 ×

https://dx.doi.org/10.1021/acs.biochem.0c00351
Biochemistry XXXX, XXX, XXX−XXX

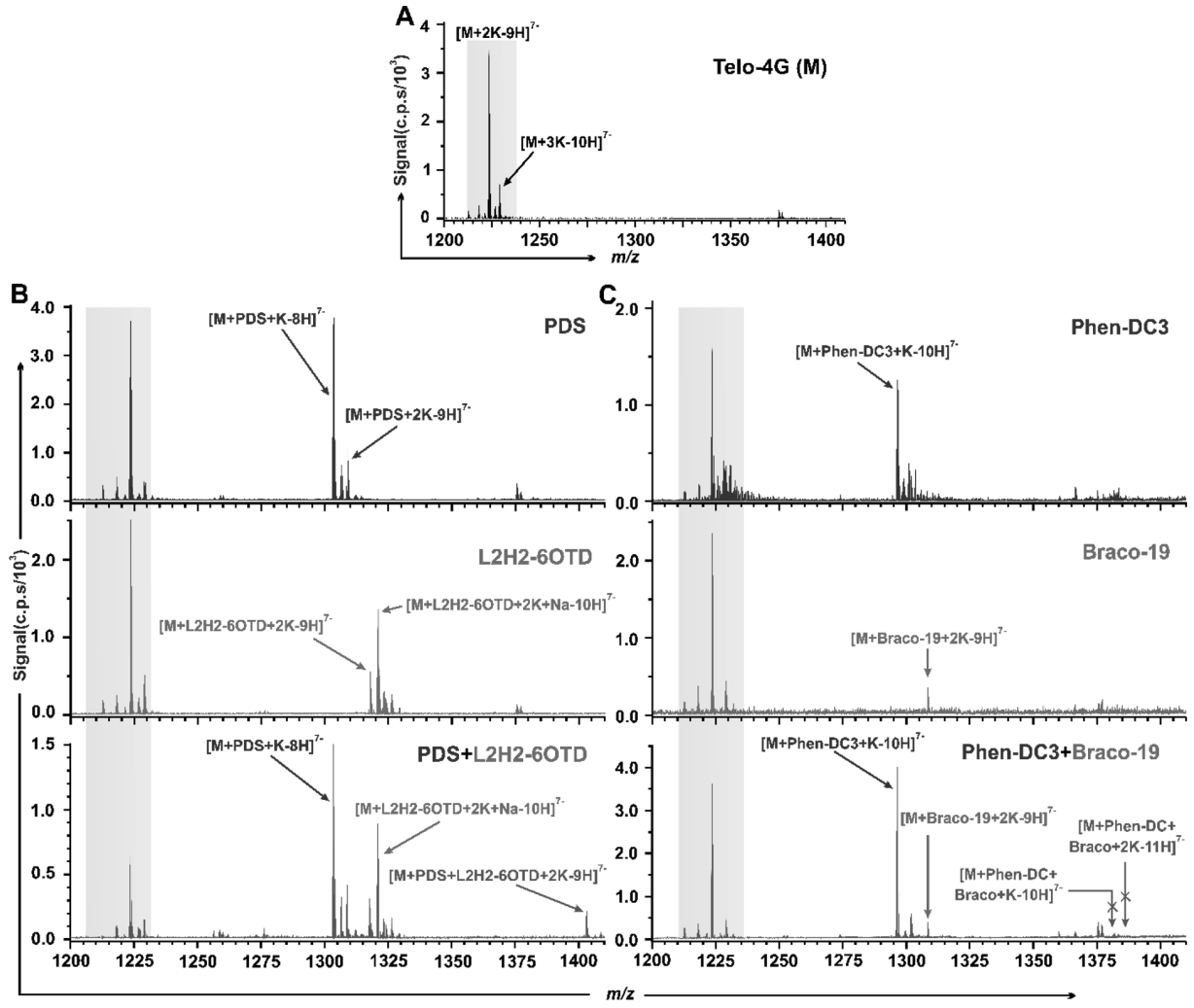

Figure 2. nESI-MS of the −7 charge state of 5 μM Telo-4G with PDS and telomestatin analogue, L2H2−6OTD, in 1 mM KCl/100 mM TMAA. (A) Mass spectrum of the Telo-4G. (B) Mass spectra of the 5 μM Telo-4G in the presence of 5 μM each of PDS (top), L2H2−6OTD (middle), and a mixture of PDS and L2H2−6OTD (bottom). Note that the −7 charge state of a complex with both ligands bound was observed at m/z 1402.2723. (C) Mass spectra of the 5 μM Telo-4G in the presence of 5 μM each of Phen-DC3 (top), Braco-19 (middle), and a mixture of Phen-DC3 and Braco-19 (bottom). Note that a complex with both ligands at m/z 1380.6908 or 1386.1130 was not detected. See Figures S3 and S4 for full mass spectra and Figures S5−S7 for blown-up mass spectra, and Table S3 for m/z values of all marked species. Shaded regions indicate Telo-4G signals without bound ligands.

10^6 ions. To ensure very high mass accuracy, found to be better than 1 mmu, the instrument was calibrated daily. All mass-spectral data were collected and processed with Xcalibur software (version 4.0, Thermo Scientific, San Jose, CA). Presented spectra show the −7 charge-state ions for the G-quadruplex and mixture of G-quadruplex with stabilizing ligands. Other detected analyte-ion charge states (e.g., −6, −8, −9, etc.) showed the same ions with the same relative distribution. See Table S3 for expected and observed m/z for major species indicated in Figure 2.

■ RESULTS AND DISCUSSION

PDS and L2H2−6OTD Show Cooperative Binding to the DNA Telomere G-Quadruplex. The 3′ human telomere overhang contains 200 ± 75 nucleotides (nts) of G-rich repeats with a consensus sequence of 5′-TTAGGG.[27] Tandem repeats of this G-rich sequence facilitate the formation of the telomeric G-quadruplex, which inhibit the interaction with the telomerase overexpressed in many tumor cells.[28] Many potent small molecules have been developed to target the DNA G-quadruplex structures formed in the telomere region.[15] In an effort to develop more effective molecules that can bind to DNA G-quadruplex, we evaluated the combination effects of different ligands. It has been found that when the G-quadruplex is bound with ligands, its thermodynamic stability often increases.[23,29] Therefore, by measuring the melting temperature (T_m) of a DNA G-quadruplex in the presence of ligands, its binding potency to G-quadruplex can be revealed. We performed CD melting for the T_m measurement. First, T_m of only a telomeric DNA G-quadruplex (Telo-4G: 5′-TTA$(GGGTTA)_4$, 5 μM) was determined as 59 °C (Figure 1B), which was followed by the T_m measurement of individual ligands (Figure 1 and Figure S2). Then, T_m of G-quadruplex in the presence of two different ligands was determined. Among the commonly used ligands, we chose some ligands that were more selective toward G-quadruplex than dsDNA, such as L2H2−6OTD (a telomestatin analogue[30]), PDS,[31] Phen-DC3,[32] and Braco-19[33] (5 μM each). We found all individual

https://dx.doi.org/10.1021/acs.biochem.0c00351
Biochemistry XXXX, XXX, XXX−XXX

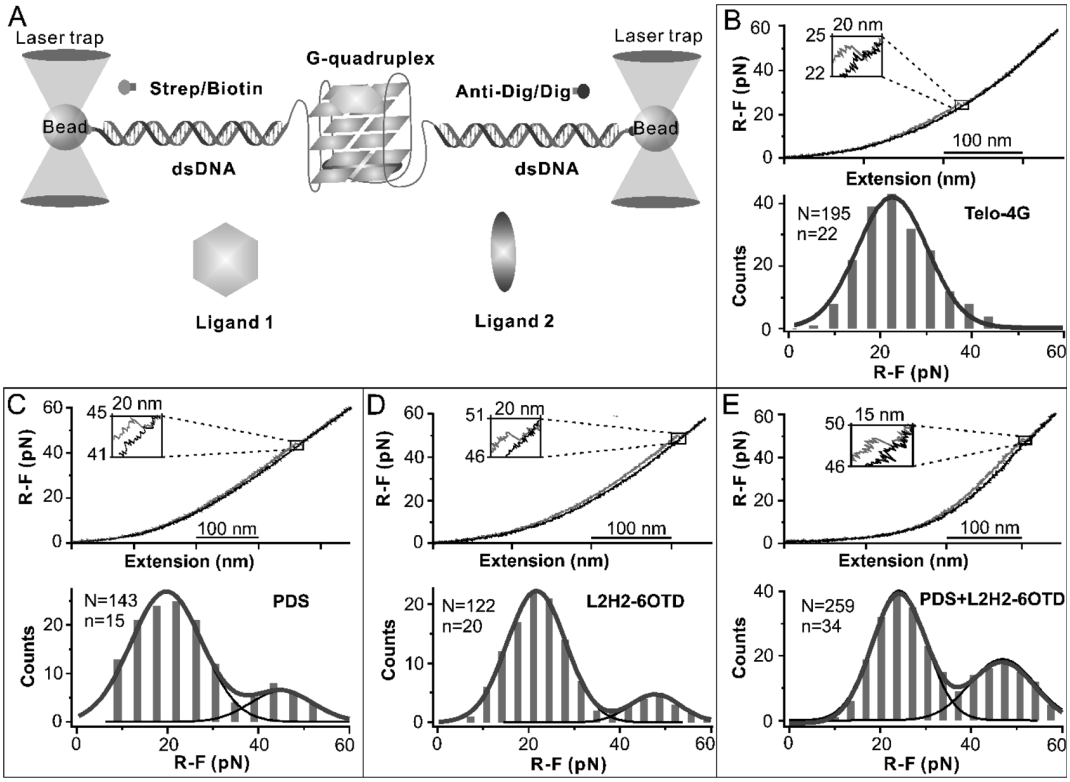

Figure 3. Experimental setup for the mechanical unfolding of the Telo-4G construct with and without ligands. (A) Single-stranded human telomeric DNA (Telo-4G) is sandwiched between two dsDNA handles. The overall construct is tethered between two optically trapped beads via an antidigoxigenin−digoxigenin and a streptavidin−biotin linkage. (B) Typical stretching (red) and relaxing (black) force−extension curves of the Telo-4G and the corresponding rupture force (R-F) histogram. Typical stretching (red) and relaxing (black) force−extension curves and the corresponding rupture force (R-F) histogram of the Telo-4G in the presence of (C) 100 nM pyridostatin (PDS), (D) 5 nM telomestatin analogue L2H2−6OTD, and (E) 100 nM PDS and 5 nM L2H2−6OTD. Solid curves depict Gaussian fittings. *N* and *n* represent the numbers of unfolding features and molecules, respectively.

ligands increased the T_m of the 5-μM DNA G-quadruplex (Figure 1B,C), indicating they all bind to the G-quadruplex. Importantly, a significantly increased T_m of 67.5 °C was obtained when both L2H2−6OTD and PDS (5 μM each) were present.

This increment (ΔT_m = 8.5 °C) was even greater than the combined ΔT_m for the two individual ligands (ΔT_m (L2H2−6OTD+PDS) = ΔT_m (L2H2−6OTD) + ΔT_m (PDS) = (3.5 + 1) °C = 4.5 °C). This result suggests the binding of both L2H2−6OTD and PDS ligands to the G-quadruplex. Further, it suggests that the binding is synergistic and cooperative: the binding of both ligands has a more pronounced effect than the additive binding of each ligand. In comparison, the T_m of G-quadruplex in the presence of the Phen-DC3 and Braco-19 ligand pair (60.5 °C) was comparable to that of individual ligand (62.5 and 61.5 °C, respectively). This observation suggests that only one ligand, either Phen-DC3 or Braco-19, binds to the telomeric G-quadruplex. The competitive nature of these two ligands may be due to the overlapping binding sites of these two ligands in the G-quadruplex structure.[34,35]

The Ternary Binding Complex Has a 1:1:1 Stoichiometric Ratio. To provide the evidence for cooperative binding of L2H2−6OTD and PDS to the G-quadruplex, we performed nanoelectrospray mass spectrometry (nESI-MS) experiments (Figure 2). Previously, Gabelica used volatile TMAA buffer to minimize nonspecific salt adducts in nESI-MS data and directly observed the stoichiometry of the ligand binding to DNA G-quadruplex.[35] Using the same buffer (1 mM KCl/100 mM TMAA, pH 6.9), we found that, in the presence of either the L2H2−6OTD or PDS ligand, there was 1:1 binding between each ligand and the G-quadruplex (Figure 2A,B). When both ligands were present, a ternary complex was observed in which the L2H2−6OTD, PDS, and telomeric G-quadruplex presented a 1:1:1 stoichiometry. This experiment directly proved the dual binding of the L2H2−6OTD and PDS to the G-quadruplex, which provides strong support for the cooperative binding observed in the CD melting experiments (Figure 1C).

As a control, when Phen-DC3 and Braco-19 were evaluated (Figure 2C), we found each ligand can bind to the telomere G-quadruplex with a 1:1 ratio. However, no MS signal was observed for the dual binding of both ligands to the G-quadruplex. This data set is in full agreement with previous CD melting results (Figure 1D) that indicate the competitive binding between Phen-DC3 and Braco-19 to the G-quadruplex.

A close inspection of the mass spectra in Figure 2B revealed that, in the presence of the L2H2−6OTD, the Na^+ adduct was observed for the telomeric G-quadruplex in addition to K^+ ions. The trace amount of Na^+ might come from the containers, the solvent, or from the quartz nanospray emitter itself that can form Na^+ adducts during the electrospray ionization process. Such an adduct was commonly observed in mass spectrometry due to the negatively charged phosphate backbone of DNA. It is known that L2H2−6OTD binds to the telomeric G-quadruplex by stacking on top of the 5′-end G-

https://dx.doi.org/10.1021/acs.biochem.0c00351
Biochemistry XXXX, XXX, XXX−XXX

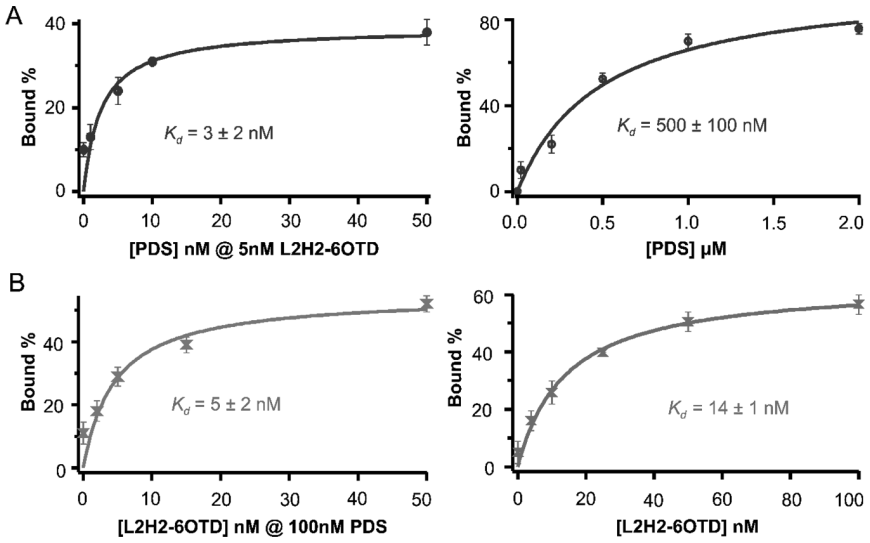

Figure 4. Binding of PDS and the telomestatin analogue, L2H2−6OTD, to the telomeric G-quadruplex is allosteric in nature. (A) Binding curves of the PDS to the G-quadruplex with (left) and without 5 nM L2H2−6OTD (right). (B) Binding curves of the L2H2−6OTD to the G-quadruplex with (left) and without 100 nM PDS (right). All experiments were performed in a 10 mM Tris buffer with 100 mM KCl at pH 7.4. A single-site binding model was used for fitting (see Supporting Information for details). Error bars are standard deviations from three independent measurements.

quartet.[36] This stacking may introduce additional interplanar space in which cations such as Na^+ has shown to fit in by simulation.[37] However, when both L2H2−6OTD and PDS bind to the G-quadruplex, the sodium ion was ejected (Figure 2B, bottom panel, see Table S4 for quantification). Such an observation indicates that binding of the second ligand, PDS, changes the interplanar space between the G-quadruplex and L2H2−6OTD, which ejects the Na^+. Similar ion ejection was observed previously by others.[35] This scenario is consistent with the allosteric binding of the two ligands to the G-quadruplex.

Cooperative Binding Has an Allosteric Nature. To investigate the mechanism of the cooperative binding of the PDS and L2H2−6OTD ligands, we employed single-molecule techniques such as mechanical unfolding and refolding of the telomere G-quadruplex.[23] Due to its superb signal-to-noise ratio, this technique has demonstrated its capability to deconvolute complex molecular interactions in a solution that contains multiple species, a feat unmatched in bulk-based techniques such as CD and NMR.[27] To this end, the same Telo-4G DNA fragment was tethered to the two optically trapped micrometer-sized polystyrene particles through affinity linkages by digoxigenin−antidigoxigenin and biotin−streptavidin interactions. For mechanical unfolding, one trapped bead was moved away from another by using a steerable mirror (see Materials and Methods).[23] This increased tension in the Telo-4G DNA, causing G-quadruplex structures to unfold.

Two rupture force (R-F) populations centered at 22 ± 2 and 45 ± 2 pN were observed (Figure 3C−E, Figures S8 and S9). The mechanical stability of telomeric G-quadruplex increases significantly due to the ligand binding, which has already been established previously.[23] Therefore, we assigned the low force population (22 pN) as a free G-quadruplex and the high force population (45 pN) as the ligand-bound G-quadruplex. The change-in-contour-length (ΔL) (Figures S10) showed average values of 8.0 ± 0.5 nm, which was consistent with folded telomere G-quadruplexes (see Supporting Information for calculation).[38] In the next step, we used two different ligands to measure mechanical stability of G-quadruplex. Again, two similar populations were observed (Figure 3C−E, Figures S8 and S9) where the 22 ± 2 pN and 45 ± 2 pN species were assigned as ligand-free and ligand-bound G-quadruplexes, respectively. The fraction of ligand-bound G-quadruplex was then estimated by the 45 ± 2 pN population. By using this method, we calculated the percentage of ligand-bound G-quadruplex in the presence of individual ligand or ligand pairs. During experiments, the concentration of each ligand was kept comparable to or below corresponding K_d value so that binding sites are not fully occupied. This provides the space for another ligand to interact with the G-quadruplex, which is instrumental in elucidating the nature of the G-quadruplex binding between two different ligands.

Comparison of dissociation constants (K_d) of one ligand to the receptor with and without another ligand allows the determination of the allostery in the binding complex.[9] As such, we measured K_d of one ligand in the presence of the other for the PDS/L2H2−6OTD ligand pair.[9] In the first experiment, we measured K_d of the PDS to the telomeric G-quadruplex in the presence of 5 nM L2H2−6OTD (designated as PDS@L2H2−6OTD; see Materials and Methods, Figure S8, and Table S1 for experimental details; see Supporting Information for the calculation of K_d). We found that the binding affinity of the PDS@L2H2−6OTD (K_d = 3 ± 2 nM; Figure 4A left) was ∼2 orders of magnitude stronger than the PDS alone (K_d = 500 ± 100 nM; Figure 4A right; see Figure S8 for unfolding histograms). Likewise, the binding affinity of the L2H2−6OTD in the presence of 100 nM PDS (L2H2−6OTD@PDS, K_d = 5 ± 2 nM; see Figure 4B left) was significantly higher than that without PDS (K_d = 14 ± 1 nM; Figure 4B right; see Figure S9 for unfolding histograms). Both experiments convincingly demonstrate an allosteric binding between PDS and L2H2−6OTD to the telomeric G-quadruplex; i.e., the presence of either of the ligand promotes the binding of the other ligand.

In Figure 4, left panel, we observed a saturation plateau (<50% occupancy) at lower ligand concentrations due to the

https://dx.doi.org/10.1021/acs.biochem.0c00351
Biochemistry XXXX, XXX, XXX−XXX

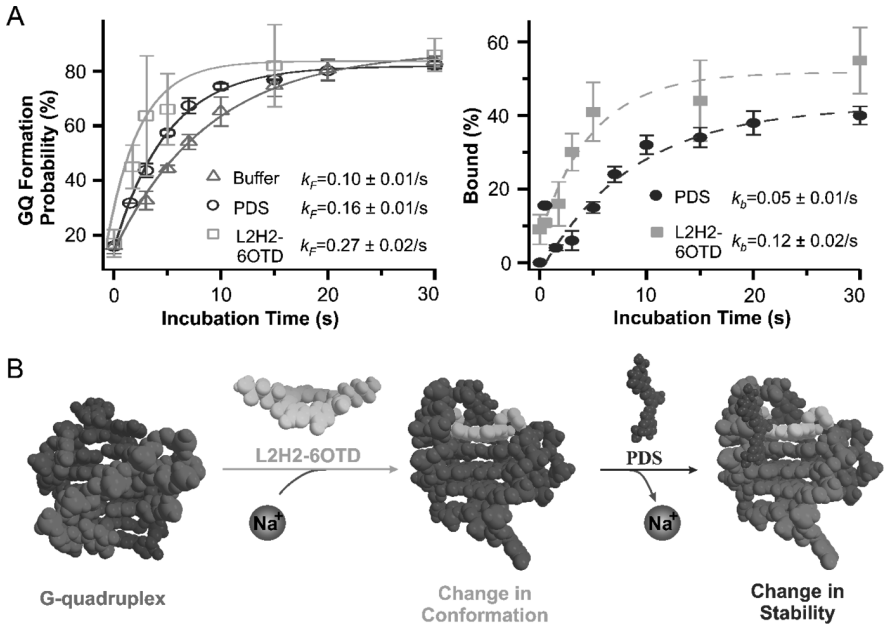

Figure 5. Sequential binding of the L2H2−6OTD and PDS to the G-quadruplex. (A) Refolding probability of all G-quadruplexes (left) and the ligand-bound G-quadruplex (right). A two-state model (see Supporting Information for details) is used for fitting to retrieve the folding/binding rate constants (k_F/k_b). Error bars are standard deviations from three measurements. (B) A schematic diagram for a possible allosteric binding mechanism, which starts with the L2H2−6OTD binding together with a Na^+ ion, followed by the PDS binding with ejection of the Na^+ ion.

tighter binding of two potent ligands. The following reasons can explain this behavior. First, before complete unfolding, the G-quadruplex structure may become loose under mechanical tension generated during the unfolding experiments. This leads to a rupture force lower than expected due to reduced binding affinity of PDS and L2H2−6OTD to the compromised G-quadruplex structure. Second, this ligand pair may bind to a particular G-quadruplex conformation. Third, the PDS and L2H2−6OTD may associate at higher concentrations, thereby reducing the magnitude of the saturation plateau.

To further investigate this allosteric binding, we performed force-pumping/force-probing (or (FP)2) experiments[23] to separately measure the binding kinetics of the PDS and the L2H2−6OTD to the telomeric G-quadruplex (Figures S11 and S12). After incubating the single Telo-4G with either PDS or L2H2−6OTD, force ramping experiments were carried out to unfold the G-quadruplex (see Materials and Methods for details). The unfolding was followed by rapid force reduction to 0 pN in 10 ms to refold the quadruplex. The refolded quadruplex was determined during a subsequent round of force ramping experiment (probing). The rupture force of the unfolding transition during the probing step reveals whether the G-quadruplex is bound with a ligand (see Figures 3, Figures S8 and S9). The G-quadruplex formation probability during incubation was calculated by the ratio of the unfolding events observed in the subsequent pulling of the same Telo-4G molecule versus the total subsequent pulling curves performed for that incubation time.

As shown in the left panel of Figure 5A, both 100 nM L2H2−6OTD (k_F = 0.27 ± 0.02 s^{-1}) and 500 nM PDS (k_F = 0.16 ± 0.01 s^{-1}) promoted the formation of G-quadruplex (k_F = 0.10 ± 0.01 s^{-1} for free G-quadruplex). After deconvoluting free G-quadruplex and ligand-bound species (Figure 5A, right), we found that the 100 nM L2H2−6OTD had a binding rate constant (k_b) of 0.12 ± 0.02 s^{-1}, while the 500 nM PDS had a k_b of 0.05 ± 0.01 s^{-1}. Given these two different concentrations, the second-order binding rate constant for the L2H2−6OTD was estimated to be 12 times faster than the PDS (1.2 × 106/M s vs 1.0 × 105/M s). Therefore, during the allosteric binding, it is likely that the L2H2−6OTD first associates with human telomeric G-quadruplex via $\pi-\pi$ stacking on the top quartet, which leads to a conformation change in the G-quadruplex, facilitating subsequent PDS binding (Figure 5B). It has been found that binding of the L2H2−6OTD can indeed change the structure of the telomeric G-quadruplex by dislocating the third loop (counted from the 5′-end).[36,39] Recent investigations also suggested that the PDS may bind to the G-quadruplex through an interaction with the two external G-quartets.[40] Thus, binding of the L2H2−6OTD to the top G-quartet[36] may render more compact stacking among three G-quartets, which leaves the bottom G-quartet more open to access the PDS in solution. On the other hand, binding of the PDS also changes the conformation of the L2H2−6OTD/G-quadruplex complex, which has been confirmed by our mass spectra data that demonstrated the ejection of the sodium ion when both L2H2−6OTD and PDS bound to the G-quadruplex (Figure 2B). Previous studies have shown that the Telo-4G sequence (5′-TTA(GGGTTA)$_4$ assumed the hybrid-1 conformation.[41] When L2H2−6OTD was bound to the same sequence, the same hybrid-1 conformation was also observed.[30,39] When we evaluated ΔL values of unfolding features, which reflected the conformation of a G-quadruplex,[41] we found they did not change during the mechanical unfolding of G-quadruplex (8.0 ± 0.5 nm) both with and without ligands (Figure S10 and Table S2). This again suggested the same G-quadruplex conformation was maintained with and without ligands. These results provide evidence for allosteric binding of heteroligands to the telomeric DNA G-quadruplex instead of conformational selection.

https://dx.doi.org/10.1021/acs.biochem.0c00351
Biochemistry XXXX, XXX, XXX−XXX

CONCLUSIONS

In summary, we have revealed that the dual binding of the PDS and L2H2−6OTD to the telomeric G-quadruplex is allosteric. We anticipate that the allosteric binding is instrumental to the design of more effective drugs targeting DNA G-quadruplexes, which have demonstrated many biological activities inside cells.

ASSOCIATED CONTENT

Supporting Information

The Supporting Information is available free of charge at https://pubs.acs.org/doi/10.1021/acs.biochem.0c00351.

Preparation of DNA construct for single-molecule experiments; evaluation of thermodynamic stability of the Telo-4G with and without ligands; full mass spectra of Telo-4G and Telo-4G with PDS; blown-up nESI-mass spectra of Telo-4G with individual ligands (PDS, L2H2−6OTD, Phen-DC3, and Braco-19) and the mixture of PDS and L2H2−6OTD; unfolding force and change-in-contour-length histograms of the Telo-4G with the L2H2−6OTD or the PDS at different concentrations; diagrams for the force-pumping/force-probing experiments during ligand binding; table for overall ligand-bound fractions by including nonunfolded features; the average change-in-contour-length (ΔL) during the mechanical unfolding of the G-quadruplex both with and without ligands; different species observed in HRMS experiments and their m/z ratios; quantification of Na^+ adducts in the ligand-bound Telo-4G species (PDF)

AUTHOR INFORMATION

Corresponding Author

Hanbin Mao − *Department of Chemistry and Biochemistry, Kent State University, Kent, Ohio 44242, United States;* orcid.org/0000-0002-6720-9429; Email: hmao@kent.edu

Authors

Shankar Pandey − *Department of Chemistry and Biochemistry, Kent State University, Kent, Ohio 44242, United States;* orcid.org/0000-0001-5576-6714

Yuanyuan Li − *Department of Chemistry and Biochemistry, Kent State University, Kent, Ohio 44242, United States; Department of Pharmacy, Daping Hospital, Army Medical University, Chongqing 400042, China*

Montwaun D. Young − *Department of Chemistry and Chemical Biology, Rensselaer Polytechnic Institute, Troy, New York 12180, United States*

Shankar Mandal − *Department of Chemistry and Biochemistry, Kent State University, Kent, Ohio 44242, United States;* orcid.org/0000-0002-2653-8760

Laichun Lu − *National Institute for Drug Clinical Trial, Beijing Tongren Hospital, Capital Medical University, Beijing 100730, China*

Jacob T. Shelley − *Department of Chemistry and Chemical Biology, Rensselaer Polytechnic Institute, Troy, New York 12180, United States*

Complete contact information is available at: https://pubs.acs.org/10.1021/acs.biochem.0c00351

Author Contributions

H.M. initiated the research, did data analyses, and gave comprehensive guidelines to the research. S.P. collected and analyzed the single-molecule data. Y.L. collected the analyzed single-molecule data. M.D.Y. did mass spectrometry. S.M. helped in synthesizing the DNA construct and single-molecule data collection. L.L. assisted in the data analysis. J.T.S. assisted in the data analysis. All authors contributed to the writing of the manuscript.

Funding

H.M. thanks NIH (1R01CA236350, for binding characterizations) and NSF (CHE-1904921, for DNA construct preparation and mechanical unfolding in laser tweezers) for research support.

Notes

The authors declare no competing financial interest.

ACKNOWLEDGMENTS

H.M. thanks prof. Kazuo Nagasawa from Tokyo University of Agriculture and Technology for L2H2-6OTD samples. J.T.S. and M.D.Y. thank prof. Daniele Fabris, Thomas Kenderdine, and Courtney L. Walton for their assistance with nESI.

REFERENCES

(1) Mergny, J. L., and Lacroix, L. (2003) Analysis of thermal melting curves. *Oligonucleotides 13*, 515−537.

(2) Whitty, A. (2008) Cooperativity and biological complexity. *Nat. Chem. Biol. 4*, 435−439.

(3) Cui, Q., and Karplus, M. (2008) Allostery and cooperativity revisited. *Protein Sci. 17*, 1295−1307.

(4) Monod, J., Changeux, J.-P., and Jacob, F. (1963) Allosteric proteins and cellular control systems. *J. Mol. Biol. 6*, 306−329.

(5) Baldwin, J., and Chothia, C. (1979) Haemoglobin: the structural changes related to ligand binding and its allosteric mechanism. *J. Mol. Biol. 129*, 175−220.

(6) Monod, J., Wyman, J., and Changeux, J.-P. (1965) On the nature of allosteric transitions: A plausible model. *J. Mol. Biol. 12*, 88−118.

(7) Koshland, D. E., Nemethy, G., and Filmer, D. (1966) Comparison of experimental binding data and theoretical models in proteins containing subunits. *Biochemistry 5*, 365−385.

(8) Motlagh, H. N., Wrabl, J. O., Li, J., and Hilser, V. J. (2014) The ensemble nature of allostery. *Nature 508*, 331−339.

(9) Casado, V., Cortes, A., Ciruela, F., Mallol, J., Ferre, S., Lluis, C., Canela, E. I., and Franco, R. (2007) Old and New Ways to Calculate the Affinity of Agonists and Antagonists Interacting with G-Protein-Coupled Monomeric and Dimeric Receptors: The Receptor−Dimer Cooperativity Index. *Pharmacol. Ther. 116*, 343−354.

(10) Peselis, A., Gao, A., and Serganov, A. (2015) Cooperativity, allostery and synergism in ligand binding to riboswitches. *Biochimie 117*, 100−109.

(11) Ricci, F., Vallée-Bélisle, A., Porchetta, A., and Plaxco, K. W. (2012) Rational Design of Allosteric Inhibitors and Activators Using the Population-Shift Model: In Vitro Validation and Application to an Artificial Biosensor. *J. Am. Chem. Soc. 134*, 15177−15180.

(12) Chen, A. G., Sudarsan, N., and Breaker, R. R. (2011) Mechanism for gene control by a natural allosteric group I ribozyme. *RNA 17*, 1967−1972.

(13) Kim, S., Broströmer, E., Xing, D., Jin, J., Chong, S., Ge, H., Wang, S., Gu, C., Yang, L., Gao, Y. Q., Su, X.-d., Sun, Y., and Xie, X. S. (2013) Probing Allostery Through DNA. *Science 339*, 816−819.

(14) Chenoweth, D. M., and Dervan, P. B. (2009) Allosteric modulation of DNA by small molecules. *Proc. Natl. Acad. Sci. U. S. A. 106*, 13175−13179.

(15) Biffi, G., Tannahill, D., McCafferty, J., and Balasubramanian, S. (2013) Quantitative visualization of DNA G-quadruplex structures in human cells. *Nat. Chem. 5*, 182−186.

(16) Siddiqui-Jain, A., Grand, C. L., Bearss, D. J., and Hurley, L. H. (2002) Direct Evidence for a G-quadruplex in a Promoter Region and Its Targeting with a Small Molecule to Repress c-*MYC* Transcription. *Proc. Natl. Acad. Sci. U. S. A. 99*, 11593−11598.
(17) Balasubramanian, S., Hurley, L. H., and Neidle, S. (2011) Targeting G-quadruplexes in Gene Promoters: a Novel Anticancer Strategy? *Nat. Rev. Drug Discovery 10*, 261−275.
(18) Goodey, N. M., and Benkovic, S. J. (2008) Allosteric regulation and catalysis emerge via a common route. *Nat. Chem. Biol. 4*, 474−482.
(19) Seok, Y.-J., Sondej, M., Badawi, P., Lewis, M. S., Briggs, M. C., Jaffe, H., and Peterkofsky, A. (1997) High Affinity Binding and Allosteric Regulation ofEscherichia coli Glycogen Phosphorylase by the Histidine Phosphocarrier Protein, HPr. *J. Biol. Chem. 272*, 26511−26521.
(20) Luchette, P., Abiy, N., and Mao, H. (2007) Microanalysis of clouding process at the single droplet level. *Sens. Actuators, B 128*, 154−160.
(21) Mao, H., and Luchette, P. (2008) An integrated laser-tweezers instrument for microanalysis of individual protein aggregates. *Sens. Actuators, B 129*, 764−771.
(22) Information obtained from UCSC Genome Bioinformatics. http://genome.ucsc.edu/.
(23) Koirala, D., Dhakal, S., Ashbridge, B., Sannohe, Y., Rodriguez, R., Sugiyama, H., Balasubramanian, S., and Mao, H. (2011) A Single-Molecule Platform for Investigation of Interactions between G-quadruplexes and Small-Molecule Ligands. *Nat. Chem. 3*, 782−787.
(24) Baumann, C. G., Smith, S. B., Bloomfield, V. A., and Bustamante, C. (1997) Ionic effects on the elasticity of single DNA molecules. *Proc. Natl. Acad. Sci. U. S. A. 94*, 6185−6190.
(25) Yu, Z., and Mao, H. (2013) Non-B DNA structures show diverse conformations and complex transition kinetics comparable to RNA or proteins–a perspective from mechanical unfolding and refolding experiments. *Chem. Rec. 13*, 102−116.
(26) Dhakal, S., Cui, Y., Koirala, D., Ghimire, C., Kushwaha, S., Yu, Z., Yangyuoru, P. M., and Mao, H. (2013) Structural and mechanical properties of individual human telomeric G-quadruplexes in molecularly crowded solutions. *Nucleic Acids Res. 41*, 3915−3923.
(27) Punnoose, J. A., Cui, Y., Koirala, D., Yangyuoru, P. M., Ghimire, C., Shrestha, P., and Mao, H. (2014) Interaction of G-Quadruplexes in the Full-Length 3′ Human Telomeric Overhang. *J. Am. Chem. Soc. 136*, 18062−18069.
(28) Jansson, L. I., Hentschel, J., Parks, J. W., Chang, T. R., Lu, C., Baral, R., Bagshaw, C. R., and Stone, M. D. (2019) Telomere DNA G-quadruplex folding within actively extending human telomerase. *Proc. Natl. Acad. Sci. U. S. A. 116*, 9350−9359.
(29) Lane, A. N., Chaires, J. B., Gray, R. D., and Trent, J. O. (2008) Stability and kinetics of G-quadruplex structures. *Nucleic Acids Res. 36*, 5482−5515.
(30) Ghimire, C., Park, S., Iida, K., Yangyuoru, P., Otomo, H., Yu, Z., Nagasawa, K., Sugiyama, H., and Mao, H. (2014) Direct Quantification of Loop Interaction and $\pi-\pi$ Stacking for G-Quadruplex Stability at the Submolecular Level. *J. Am. Chem. Soc. 136*, 15537−15544.
(31) Rodriguez, R., Müller, S., Yeoman, J. A., Trentesaux, C., Riou, J.-F., and Balasubramanian, S. (2008) A Novel Small Molecule That Alters Shelterin Integrity and Triggers a DNA-Damage Response at Telomeres. *J. Am. Chem. Soc. 130*, 15758−15759.
(32) De Cian, A., DeLemos, E., Mergny, J.-L., Teulade-Fichou, M.-P., and Monchaud, D. (2007) Highly Efficient G-Quadruplex Recognition by Bisquinolinium Compounds. *J. Am. Chem. Soc. 129*, 1856−1857.
(33) Burger, A. M., Dai, F. P., Schultes, C. M., Reszka, A. P., Moore, M. J., Double, J. A., and Neidle, S. (2005) The G-quadruplex-interactive molecule BRACO-19 inhibits tumor growth, consistent with telomere targeting and interference with telomerase function. *Cancer Res. 65*, 1489−1496.
(34) Machireddy, B., Sullivan, H.-J., and Wu, C. (2019) Binding of BRACO19 to a telomeric G-quadruplex DNA probed by all-atom molecular dynamics simulations with explicit solvent. *Molecules 24*, 1010.
(35) Marchand, A., Granzhan, A., Iida, K., Tsushima, Y., Ma, Y., Nagasawa, K., Teulade-Fichou, M.-P., and Gabelica, V. (2015) Ligand-Induced Conformational Changes with Cation Ejection upon Binding to Human Telomeric DNA G-Quadruplexes. *J. Am. Chem. Soc. 137*, 750−756.
(36) Chung, W. J., Heddi, B., Tera, M., Iida, K., Nagasawa, K., and Phan, A. T. (2013) Solution structure of an intramolecular (3+ 1) human telomeric G-quadruplex bound to a telomestatin derivative. *J. Am. Chem. Soc. 135*, 13495−13501.
(37) Rosu, F., Gabelica, V., Smargiasso, N., Mazzucchelli, G., Shin-Ya, K., and De Pauw, E. (2010) Cation involvement in telomestatin binding to g-quadruplex DNA. *J. Nucleic Acids 2010*, 1.
(38) Punnoose, J. A., Cui, Y., Koirala, D., Yangyuoru, P. M., Ghimire, C., Shrestha, P., and Mao, H. (2014) Interaction of G-Quadruplexes in the Full-Length 3′ Human Telomeric Overhang. *J. Am. Chem. Soc. 136*, 18062−18069.
(39) Jonchhe, S., Ghimire, C., Cui, Y., Sasaki, S., McCool, M., Park, S., Iida, K., Nagasawa, K., Sugiyama, H., and Mao, H. (2019) Binding of a Telomestatin Derivative Changes Mechanical Anisotropy of Human Telomeric G-Quadruplex. *Angew. Chem., Int. Ed. 58*, 877−881.
(40) Le, D. D., Di Antonio, M., Chan, L. K. M., and Balasubramanian, S. (2015) G-quadruplex ligands exhibit differential G-tetrad selectivity. *Chem. Commun. 51*, 8048−8050.
(41) Yu, Z., Koirala, D., Cui, Y., Easterling, L. F., Zhao, Y., and Mao, H. (2012) Click Chemistry Assisted Single-Molecule Fingerprinting Reveals a 3D Biomolecular Folding Funnel. *J. Am. Chem. Soc. 134*, 12338−12341.

https://dx.doi.org/10.1021/acs.biochem.0c00351
Biochemistry XXXX, XXX, XXX−XXX